

Making the \mathcal{PT} symmetry unbreakable

Vitaly Lutsky¹, Eitam Luz¹, Er'el Granot², and Boris A. Malomed^{1,3,4}

¹*Department of Physical Electronics, School of Electrical Engineering,
Faculty of Engineering, Tel Aviv University, Tel Aviv 69978, Israel*

²*Department of Electrical and Electronic Engineering, Ariel University, Ariel, Israel*

³*Center for Light-Matter Interaction, Tel Aviv University, Tel Aviv 69978, Israel*

⁴*ITMO University, St.Petersburg 197101, Russia*

It is well known that typical \mathcal{PT} -symmetric systems suffer symmetry breaking when the strength of the gain-loss terms, i.e., the coefficient in front of the non-Hermitian part of the underlying Hamiltonian, exceeds a certain critical value. In this article, we present a summary of recently published and newly produced results which demonstrate various possibilities of extending the \mathcal{PT} symmetry to arbitrarily large values of the gain-loss coefficient. First, we recapitulate the analysis which demonstrates a possibility of the restoration of the \mathcal{PT} symmetry and, moreover, complete avoidance of the breaking in a photonic waveguiding channel of a subwavelength width. The analysis is necessarily based on the system of Maxwell's equations, instead of the usual paraxial approximation. Full elimination of the \mathcal{PT} -symmetry-breaking transition is found in a deeply subwavelength region. Next, we review a recently proposed possibility to construct stable one-dimensional (1D) \mathcal{PT} -symmetric solitons in a paraxial model with arbitrarily large values of the gain-loss coefficient, provided that the self-trapping of the solitons is induced by self-defocusing cubic nonlinearity, whose local strength grows sufficiently fast from the center to periphery. The model admits a particular analytical solution for the fundamental soliton, and provides full stability for families of fundamental and dipole solitons. It is relevant to stress that this model is nonlinearizable, hence the concept of the \mathcal{PT} symmetry in it is also an essentially nonlinear one. Finally, we report new results for unbreakable \mathcal{PT} -symmetric solitons in 2D extensions of the 1D model: one with a quasi-1D modulation profile of the local gain-loss coefficient, and another with the fully-2D modulation. These settings admit particular analytical solutions for 2D solitons, while generic soliton families are found in a numerical form. The quasi-1D modulation profile gives rise to a stable family of single-peak 2D solitons, while their dual-peak counterparts tend to be unstable. The soliton stability in the full 2D model is possible if the local gain-loss term is subject to spatial confinement.

I. INTRODUCTION

A fundamental principle of the quantum theory is that, while the underlying wave function may be complex, eigenvalues of energy and other physically relevant quantities must be real, which is provided by the condition that the respective Hamiltonian is self-conjugate (Hermitian) [1]. On the other hand, the condition of the reality of the entire energy spectrum does not necessarily imply that it is generated by a Hermitian Hamiltonian. Indeed, it had been demonstrated, about twenty years ago, that non-Hermitian Hamiltonians obeying the parity-time (\mathcal{PT}) symmetry may also produce entirely real spectra [2–8]. In terms of the usual single-particle Hamiltonian, which includes potential $U(\mathbf{r})$, the \mathcal{PT} symmetry implies that the potential is complex, $U(\mathbf{r}) = V(\mathbf{r}) + iW(\mathbf{r})$ (the usual Hermitian Hamiltonian contains a strictly real potential), its real and imaginary parts being, respectively, even and odd functions of coordinates [2]:

$$V(\mathbf{r}) = V(-\mathbf{r}), W(-\mathbf{r}) = -W(\mathbf{r}), \text{ i.e., } U(-\mathbf{r}) = U^*(\mathbf{r}), \quad (1)$$

where $*$ stands for the complex conjugate. For a given real part of the potential, the spectrum of \mathcal{PT} -symmetric models remains completely real, i.e., physically relevant, as long as the strength of the imaginary component of the potential is kept below a certain critical value, which is a threshold of the \mathcal{PT} -symmetry breaking, above which the system becomes unstable. The loss of the \mathcal{PT} symmetry may be preceded by the onset of the jamming anomaly, which means transition from increase to decreases of the power flux between the gain and loss elements in the system following the increase of the gain-loss coefficient [9, 10]. It is relevant to mention that some relatively simple \mathcal{PT} -symmetric systems may be explicitly transformed into an alternative form admitting a representation in terms of an Hermitian Hamiltonian [11, 12].

While the concept of \mathcal{PT} -symmetric Hamiltonians remained an abstract one in the framework of the quantum theory per se, theoretical works had predicted a possibility to emulate this concept in optical media with symmetrically placed gain and loss elements [13]–[26], making use of the commonly known similarity between the Schrödinger equation in quantum mechanics and the classical equation governing the paraxial light propagation in classical waveguides. These predictions were followed by the implementation in optical waveguiding settings of various types [27]–[30], as well as in metamaterials [31], lasers [32] (and laser absorbers [33]), microcavities [34], optically induced atomic lattices [35],

exciton-polariton condensates [36]-[38], and in other physically relevant contexts. In particular, the transitions from unbroken to broken \mathcal{PT} symmetry was observed in many experiments. One of prominent experimentally demonstrated applications of the \mathcal{PT} symmetry in optics is unidirectional transmission of light [39].

Other classical waveguiding settings also admit emulation of the \mathcal{PT} symmetry, as demonstrated in acoustics [40] and predicted in optomechanical systems [41]. Also predicted were realizations of this symmetry in atomic Bose-Einstein condensates [42], magnetism [43], mechanical chains of coupled pendula [44], and electronic circuits [45] (in the latter case, the prediction was also demonstrated experimentally). In terms of the theoretical analysis, \mathcal{PT} -symmetric extensions were also elaborated for Korteweg - de Vries [46, 47], Burgers [48], and sine-Gordon [49] equations, as well as in a system combining the \mathcal{PT} symmetry with the optical emulation of the spin-orbit coupling [50].

While the \mathcal{PT} symmetry is a linear property of the system, it may be naturally combined with intrinsic nonlinearity of the medium in which the symmetry is realized, such as the ubiquitous Kerr nonlinearity of optical waveguides. Most typically, these settings are modelled by nonlinear Schrödinger equations (NLSEs) with the \mathcal{PT} -symmetric potentials, subject to constraint (1), and cubic terms. Such models may give rise to \mathcal{PT} -symmetric solitons, which were considered, chiefly theoretically, in a large number of works (see, in particular, theoretical papers [15], [19]-[25] and recent reviews [51, 52]), and experimentally demonstrated too [30]. While most of these works were dealing with one-dimensional (1D) models, stable \mathcal{PT} -symmetric solitons were also found in some two-dimensional (2D) models [23], [53]-[58], [50]. A characteristic feature of solitons in \mathcal{PT} -symmetric systems is that, although these systems model, generally speaking, dissipative dynamics (the systems have no dynamical invariants), their solitons form continuous families like in conservative systems (defined by usual Hermitian Hamiltonians) [59], while traditional dissipative nonlinear systems normally give rise to isolated solutions in the form of dissipative solitons, which do not form families (if a dissipative soliton is stable, it plays the role of an attractor in the system's dynamics [60]-[62]).

Similar to their linear counterparts, soliton states are also subject to destabilization via the breaking of the \mathcal{PT} symmetry at a critical value of the strength of the gain-loss terms [63]. Nevertheless, there are specific models which make the solitons' \mathcal{PT} symmetry *unbreakable*, extending it to arbitrarily large values of the gain-loss strength, i.e., the coefficient in front of the non-Hermitian part of the respective Hamiltonian [64]-[66]. The particular property of those models is that self-trapping of solitons is provided not by the usual self-focusing sign of the cubic nonlinearity, but by the opposite defocusing sign, with the local strength of the self-defocusing growing fast enough from the center to periphery. For conservative systems (in the absence of gain and loss), this scheme of the self-trapping of stable 1D, 2D, and 3D solitons was elaborated previously in a number of works [67]-[77].

The objective of the present article is to provide a brief survey of systems which may support unbreakable \mathcal{PT} symmetry, as this property is quite promising for potential applications, and is interesting in its own right. It was recently elaborated in two completely different settings. One is the above-mentioned model with the solitons supported by the spatially growing strength of local self-defocusing. On the other hand, a possibility of creating the \mathcal{PT} symmetry persisting up to indefinitely large values of the gain-loss coefficient was also discovered in the context of nanophotonics, considering light propagation in structures combining refractive, amplifying, and attenuating elements at a subwavelength scale [78]. This setting was theoretically analyzed in a purely linear form, with an essential peculiarity that the corresponding model is, naturally, based on the full system of Maxwell's equations, rather than the paraxial-propagation equation of the Schrödinger type, which was used in an absolute majority of works dealing with the \mathcal{PT} symmetry in optical media. Basic findings for the restoration of the \mathcal{PT} symmetry, and a possibility of making it completely unbreakable in the linear nanophotonic model are presented below in Section II.

The results for unbreakable 1D \mathcal{PT} -symmetric solitons in the model based on the paraxial-propagation NLSE with the spatially growing strength of the self-defocusing nonlinearity are summarized in Section III. It is followed by Section IV, which reports *new results* for 2D extensions of the unbreakable \mathcal{PT} symmetry in a nonlinear model of a similar type. We consider two different versions of the 2D system, with the quasi-one-dimensional or fully two-dimensional \mathcal{PT} symmetry, the former meaning that the gain and loss are swapped by reflection $x \Leftrightarrow -x$, while the reflection in the perpendicular direction, $y \Leftrightarrow -y$ leaves the gain-loss pattern invariant. The main issue is the stability of the 2D \mathcal{PT} -symmetric solitons, which turn out to be essentially more stable in the case of the quasi-1D symmetry than in the framework of the full 2D scheme. An essential asset of the 1D, quasi-1D, and full 2D models is that a number of soliton solutions can be obtained in an exact analytical form, even if not all of them are stable.

II. RESTORATION AND PERSISTENCE OF THE \mathcal{PT} SYMMETRY IN THE PHOTONIC MEDIUM WITH A SUBWAVELENGTH STRUCTURE

Following Ref. [78], we here consider the propagation of monochromatic light beams with the TM (transverse-magnetic) polarization, which include only \mathcal{E}_x , \mathcal{E}_z , and \mathcal{H}_y components of the electric and magnetic fields. The propagation is considered along the z axis in an effectively 2D medium whose dielectric permittivity is modulated in the transverse direction, x . The spatial evolution of the field components is governed by the reduced system of the

Maxwell's equations:

$$\begin{aligned}
i \frac{\partial E_x}{\partial z} &= -\frac{1}{\varepsilon_0 \omega} \frac{\partial}{\partial x} \left(\frac{1}{\varepsilon_{\text{rel}}} \frac{\partial \mathcal{H}_y}{\partial x} \right) - \mu_0 \omega \mathcal{H}_y, \\
i \frac{\partial \mathcal{H}_y}{\partial z} &= -\varepsilon_0 \varepsilon_{\text{rel}} \omega \mathcal{E}_x, \\
\mathcal{E}_z &= \frac{i}{\varepsilon_0 \varepsilon_{\text{rel}} \omega} \frac{\partial \mathcal{H}_y}{\partial x},
\end{aligned} \tag{2}$$

where ω is the frequency of the monochromatic carrier, ε_0 and μ_0 are the vacuum permittivity and permeability, and $\varepsilon_{\text{rel}} = \varepsilon_{\text{bg}} + \varepsilon^{\text{re}}(x) + i\varepsilon^{\text{im}}(x)$ is the complex relative permittivity of the \mathcal{PT} -symmetric structure, with x -dependent real and imaginary parts, added to the background permittivity, ε_{bg} .

Two different modulation patterns were considered in Ref. [78], corresponding, respectively, to a single waveguiding channel or a periodic guiding structure in the (x, z) plane. In this article, we focus on solitary (localized) modes, therefore only the former pattern is explicitly considered. It is defined by the following transverse (x -dependent) profile:

$$\varepsilon_{\text{rel}}(x) = \varepsilon_{\text{bg}} + \text{sech}^2 \left(\frac{x}{d} \right) \left[p + i\alpha \sinh \left(\frac{x}{d} \right) \right], \tag{3}$$

where d and $p > 0$ represent, severally, the width and depth of the guiding channel, while $\alpha > 0$ is the strength of the gain-loss term. In accordance with the the general definition of the \mathcal{PT} symmetry, the real and imaginary parts of the profile are even and odd functions of x , respectively, cf. Eq. (1).

Eigenmodes for subwavelength beams with propagation constant b are looked for as solutions to Eq. (2) in the form of

$$\{\mathcal{E}_x(x, z), \mathcal{H}_y(x, z), \mathcal{E}_z(x, z)\} = e^{ibz} \{E_x(x)H_y(x), E_z(x)\}. \tag{4}$$

Numerical solution of Eq. (2) with modulation profile (3) has produced three types of the solutions [78]: (i) ones with real $b > \sqrt{\varepsilon_{\text{bg}}}$ represent stable \mathcal{PT} -symmetric beams guided by the channel; (ii) solutions with a complex propagation constant, which has $\text{Re}(b) > \sqrt{\varepsilon_{\text{bg}}}$, $\text{Im}(b) \neq 0$ represent, as it follows from Eq. (4), exponentially growing (unstable) channel-guided modes with broken \mathcal{PT} symmetry, and (iii) delocalized modes, which are not actually guided by the channel, have $\text{Re}(b) < \sqrt{\varepsilon_{\text{bg}}}$.

The situation which occurs in a majority of previously studied models is that, with the increase of the gain-loss strength, α , the \mathcal{PT} symmetry of the guided states suffers breaking at a critical value, α_{cr} . This is indeed observed in the present case in the nearly-paraxial regime, namely, at $d/\lambda \gtrsim 1/5$, where λ is the underlying wavelength of the optical beam (below, following Ref. [78], particular results are displayed for $\lambda = 632.8$ nm (visible red), and $\varepsilon_{\text{bg}} = 2.25$). In particular, at $d = 120$ nm, the breaking of the \mathcal{PT} symmetry takes place at $\alpha_{\text{cr}} \approx 1.95$, see Fig. 1(a) (in Fig. 1, the \mathcal{PT} symmetric modes exist at a single value of the propagation constant, as the underlying wavelength is fixed). However, in the deeply subwavelength situation, corresponding to essentially smaller channel's widths, such as $d = 60$ nm $\simeq \lambda/10$ and 30 nm $\simeq \lambda/20$ (see Figs. 1(b,c)), a drastically different situation is observed: in the former case, the breaking of the \mathcal{PT} symmetry is followed its *restoration* at still larger values of α , and in the latter case the breaking *does not happen* at all.

It is relevant to mention that a similar effect of the spontaneous restoration of the \mathcal{PT} symmetry, although not the full elimination of the symmetry breaking, was reported too in some other models (based on the paraxial, rather than subwavelength, equations), including a linear discrete system of the Aubry-André type [79], and a nonlinear model based on the NLSE in 1D [80]. Examples of unbreakable \mathcal{PT} symmetry are known too in simple models with few degrees of freedom, such as a \mathcal{PT} dimer [11].

A set of typical eigenmodes of the electromagnetic fields, which correspond, respectively, to the unbroken, broken, and restored \mathcal{PT} symmetry, are displayed in Fig. 2. It is clearly seen that, in the case of the unbroken and restored symmetry, each field component is either spatially even or odd, while the modal spatial (anti)symmetry is broken too when the \mathcal{PT} symmetry does not hold.

Finally, the results of the consideration of the model are summarized in Fig. 3, which shows regions of the unbroken, broken, and restored \mathcal{PT} symmetry in the plane of the essential control parameters, *viz.*, the gain-loss coefficient, α , and the width of the guiding channel, d . Relatively small areas where no guided modes exist (in the latter case, the optical beam coupled into the channel waveguide suffers delocalization, spreading out into the entire (x, z) plane) are shown too. The conclusion suggested by Fig. 3 is quite clear: in the near-paraxial regime, corresponding to a relatively broad guiding channel, with $d \gtrsim 120$ nm, the usual scenario of the \mathcal{PT} -symmetry breaking, following the increase of α , is observed. However, in the deeply subwavelength region, the symmetry (hence, the stability of the guided modes too) is either readily *restored* with the further increase of α , or is *never broken*. Figure 3 demonstrates

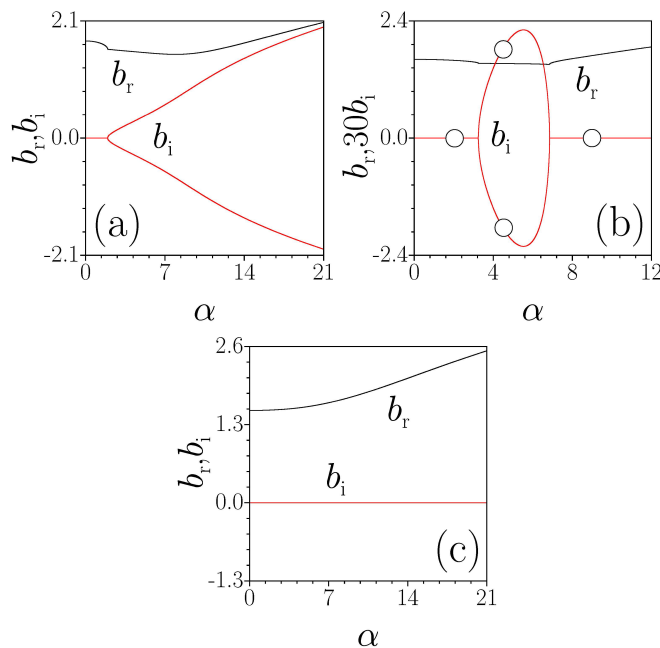


FIG. 1: Real and imaginary parts of the propagation constant, b_r and b_i , versus the gain-loss strength, α , in Eq. (3), for the guiding channel with depth $p = 1.7$, and widths $d = 120$ nm (a), $d = 60$ nm (b), and $d = 30$ nm (c) (as per Ref. [78]). Circles in panel (b) designate examples of the eigenmodes displayed in Fig. 2. The underlying wavelength is $\lambda = 632.8$ nm, and the background dielectric permeability is $\varepsilon_{\text{bg}} = 2.25$. The emergence of b_i in panels (a) and (b) signals the breaking of the \mathcal{PT} symmetry, while the disappearance of b_i in (b) implies the *restoration* of the symmetry. In the case shown in (c), the \mathcal{PT} symmetry is *never broken*.

too that region **3** of the unbroken and restored stability tends to expand, although not very dramatically, with the increase of the channel's depth, p (see Eq. 3)), while, quite naturally, the delocalization area **2** shrinks.

III. UNBREAKABLE \mathcal{PT} -SYMMETRIC SOLITONS IN ONE DIMENSION

The 1D model which is capable to support solitons with unbreakable \mathcal{PT} symmetry by means of the self-defocusing nonlinearity with the local strength, $S(\eta)$, growing from the center to infinity, as a function of coordinate η , is based on the NLSE for the amplitude of the electromagnetic field, u [64]:

$$i\frac{\partial u}{\partial \xi} + \frac{1}{2}\frac{\partial^2 u}{\partial \eta^2} - S(\eta)|u|^2 u = -iR(\eta)u, \quad (5)$$

where ξ is the propagation coordinate, and $S(\eta)$ provides for the self-trapping of 1D solitons under that condition that $S(\eta)$ grows faster than $|\eta|$ at $|\eta| \rightarrow \infty$ [68, 71]. Here, following Ref. [64], we adopt a steep anti-Gaussian modulation profile,

$$S(\eta) = (1 + \sigma\eta^2) \exp\left(\frac{1}{2}\eta^2\right), \quad (6)$$

where coefficients equal to 1 and 1/2 may be fixed to these values by means of rescaling of a more general expression. Further, the spatially-odd gain-loss modulation profile is adopted also as it was done in Ref. [64]:

$$R(\eta) = \beta\eta \exp(-\Gamma\eta^2), \quad (7)$$

with $\beta > 0$ and $\Gamma \geq 0$.

An advantage of fixing the profiles in the form of Eqs. (6) and (7) is that they admit a particular exact solution for the self-trapped \mathcal{PT} -symmetric soliton [64], provided that $\Gamma = 0$ is set in Eq. (7):

$$u(\eta, \xi) = \frac{1}{2\sqrt{2\sigma}} \exp\left(ib\xi - 2i\beta\eta - \frac{1}{4}\eta^2\right), \quad (8)$$

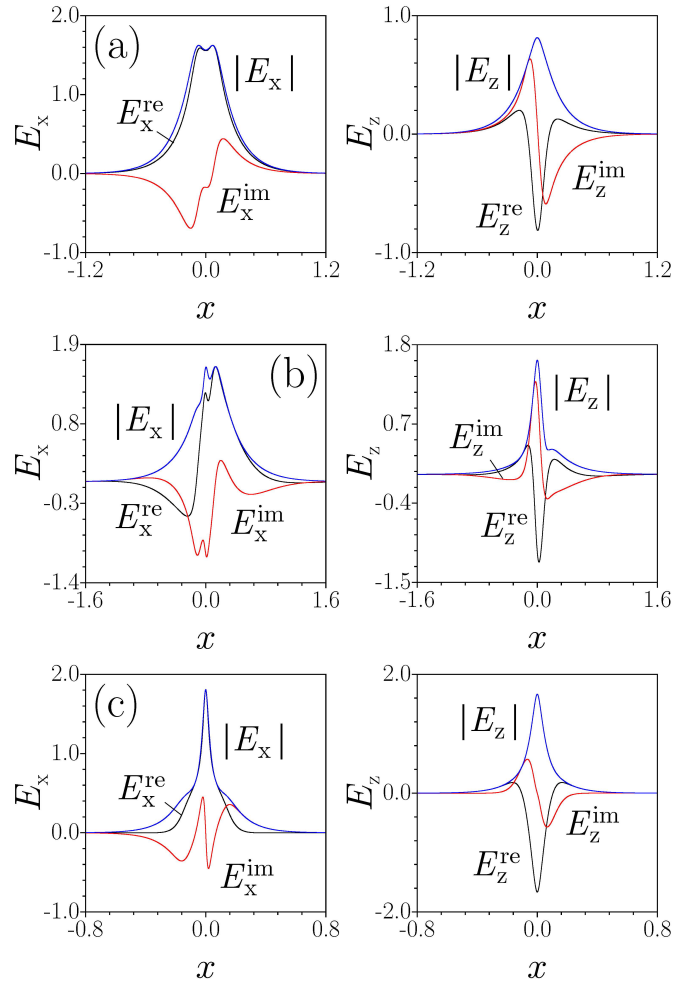


FIG. 2: Profiles of the guided modes designated by circles in Fig. 1, at $\alpha = 2.0$ (a), 4.5 (b), and 9.5 (c), which are typical modes with unbroken, broken, and *restored* \mathcal{PT} symmetry, respectively (as per Ref. [78]). The fields are plotted in dimensionless units, while transverse coordinate x is measured in μm .

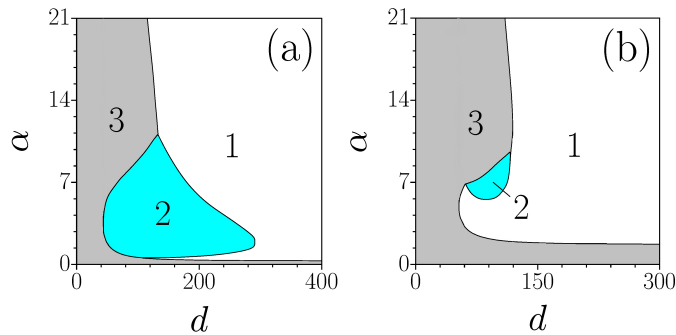


FIG. 3: Domains of the existence and stability of the \mathcal{PT} -symmetric modes guided by channel (3), in the plane of the channel's width, d , and gain-loss coefficient, α (as per Ref. [78]). The depth of the channel is $p = 0.3$ in (a), which represents a shallow conduit, and $p = 1.7$ in (b), representing a deep one. The symmetry is broken in region **1**, and unbroken or *restored* in region **3**, respectively, while region **2** does not support any localized mode.

at a single value of the propagation constant:

$$b = - \left(2\beta^2 + \frac{1}{4} + \frac{1}{8\sigma} \right). \quad (9)$$

The availability of the exact solution is principally important for establishing the concept of the *unbreakability* of the \mathcal{PT} symmetry: obviously, the solution given by Eqs. (8) and (9) exist for *arbitrarily large* values of the gain-loss strength, β , there being no critical value beyond which solitons would not exist. Moreover, in Ref. [64] it was checked, at least in a part of the parameter plane (β, σ) , that the exact solitons are stable.

It is relevant to stress that the model with the sufficiently quickly growing nonlinearity coefficient $S(\eta)$ is *nonlinearizable*: the form of decaying tails of generic self-trapped modes can be investigated analytically (it turns out to be the same as in the particular exact solution (8)), but it is necessary to keep the nonlinear term in Eq. (5) for this purpose [67, 68]. Accordingly, the linear spectrum of the present model cannot be defined, the respective concept of the \mathcal{PT} symmetry and its breaking or unbreakability being a nonlinear one too. The same pertains to the 2D model considered in the next section.

Numerical solution of Eq. (5) produces many families of complex solitons with real propagation constant b , in the form of

$$u(\eta, \xi) = \exp(ib\xi) [w_r(\eta) + iw_i(\eta)], \quad (10)$$

which may be naturally identified as fundamental solitons, dipoles, tripoles, quadrupoles, and so on. These solution types feature profiles of $|w(\eta)| \equiv \sqrt{w_r^2(\eta) + w_i^2(\eta)}$ with, respectively, one, two, three, etc. peaks (local maxima). Solitons are characterized by their integral power,

$$U = \int_{-\infty}^{+\infty} |w(\eta)|^2 d\eta. \quad (11)$$

Characteristic examples of stable fundamental and dipole solutions are displayed in Fig. 4 (they were obtained for $\sigma = 0$, in which case exact soliton (8) does not exist, but numerically found solitons are available and may be stable). It is seen that the increase of the gain-loss coefficient, β , makes the shape of the solitons more complex, but the fundamental and dipole solitons remain fully stable as long as they exist, while higher-order tripoles and quadrupoles have both stability and instability areas [64] (as briefly shown in Fig. 5(b)).

Most essential results characterizing the behavior of solitons in the present model are collected in Fig. 5. In particular, Fig. 5(a) shows that, at fixed b , branches of the fundamental and dipole solitons, remaining completely stable, merge and disappear, with the increase of the gain-loss coefficient, β , at a critical (“upper”) value, which is $\beta_{\text{upp}} \approx 2.135$ in Fig. 5(a). However, stable fundamental and dipole soliton can be found at arbitrarily high values of β , as demonstrated by the lower curve in Fig. 5(c), which shows the critical value β_{upp} vs. b : obviously, β may become indefinitely large with the increase of $|b|$. In addition, the upper curve shows the growth with $|b|$ of a similar critical (“upper”) value at which another pair of solitons, *viz.*, tripoles and quadrupoles, merge, as can be seen in Fig. 5(b) (however, unlike the fundamental and dipole modes, the tripole and quadrupole branches become unstable prior to the merger, as seen in 5(b)).

IV. UNBREAKABLE \mathcal{PT} -SYMMETRIC SOLITONS IN TWO DIMENSIONS

A. The model and analytical solutions

Results presented in the above sections summarize findings originally published in Refs. [78] and [64], respectively. Here we report previously unpublished analytical and numerical results obtained for 2D generalizations of the model based on Eq. (5). The 2D model with transverse coordinates (x, y) and propagation distance z is based on the following NLSE for the amplitude of the electromagnetic field, $w(x, y, z)$:

$$i \frac{\partial w}{\partial z} + \frac{1}{2} \left(\frac{\partial^2 w}{\partial x^2} + \frac{\partial^2 w}{\partial y^2} \right) - S(r) |w|^2 w = iR(x, y) w, \quad (12)$$

where $r \equiv \sqrt{x^2 + y^2}$ is the radial coordinate, and the nonlinearity-modulation profile is chosen similar to its 1D counterpart (6):

$$S(r) = (1 + \sigma r^2) \exp(r^2), \quad (13)$$

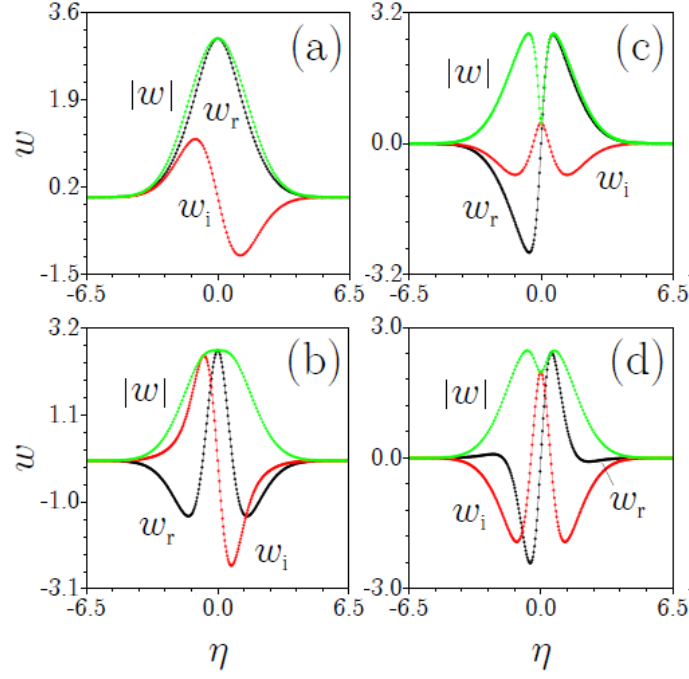


FIG. 4: Profiles of fundamental (a),(b) and dipole (c),(d) stable one-dimensional solitons, found as numerical solutions of Eq. (5) with $\sigma = 0$ and $\gamma = 1/2$, for a fixed value of the propagation constant, $b = -10$ (as per Ref. [64]). Panels (a), (c) and (b), (d) pertain, severally, to $\beta = 1.04$ and 3.47 .

with $\sigma \geq 0$.

Here we consider two different versions of the gain-loss spatial profile: a quasi-1D one, symmetric only with respect to x :

$$R(x, y) = \beta_0 x \exp(-\Gamma r^2), \quad (14)$$

and a profile symmetric with respect to x and y , which may be called a fully 2D one:

$$R(x, y) = \beta_0 xy \exp(-\Gamma r^2), \quad (15)$$

with constants $\Gamma \geq 0$ and $\beta_0 > 0$.

Stationary solutions with a real propagation constant, b , are looked for as

$$w(x, y) = \exp(ibz) W(x, y), \quad (16)$$

with complex function $W(x, y)$ satisfying the following equation:

$$bW = \frac{1}{2} \left(\frac{\partial^2 W}{\partial x^2} + \frac{\partial^2 W}{\partial y^2} \right) - S(r)|W|^2 W - iR(x, y)W. \quad (17)$$

In the case of $\Gamma = 0$ in Eqs. (14) and (15), Eq. (17), with σ and $R(x, y)$ taken in the form of Eqs. (13) and (14), gives rise to an exact analytical solution:

$$W(x, y) = W_0 \exp\left(-\frac{1}{2}r^2 - i\beta_0 x\right), \quad (18)$$

(cf. the 1D solution (8)), with

$$W_0^2 = \frac{1}{2\sigma}, \quad b = -\left(1 + \frac{\beta_0^2}{2} + \frac{1}{2\sigma}\right). \quad (19)$$

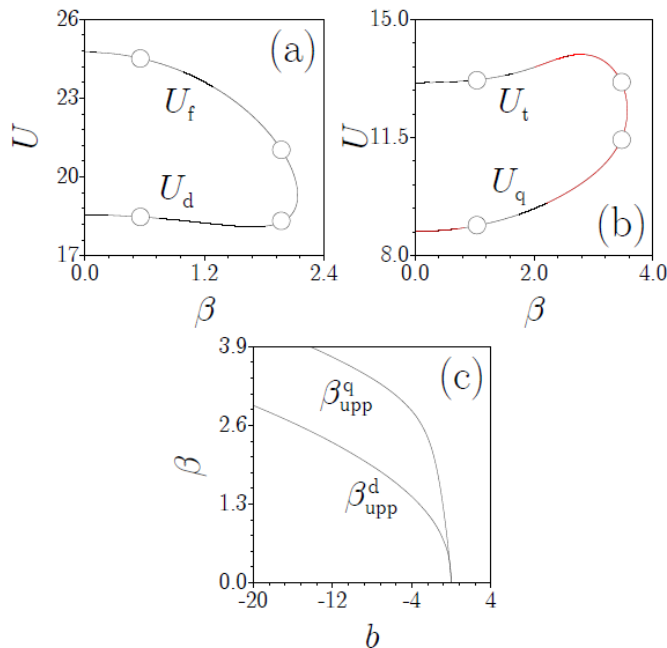


FIG. 5: The solitons' integral power, defined in Eq. (11), vs. the gain-loss strength, β , for branches of the fundamental and dipole solitons (a), and ones of the tripole and quadrupole types (b) (as per Ref. [64]). In (b), black and red segments designate stable and unstable solitons, respectively (the fundamental and dipole solitons are completely stable in their existence areas). Circles in (a) correspond to examples of the solutions shown in Fig. 4 (circles in (b) correspond to examples of stable and unstable tripole and quadrupole solitons which can be found in Ref. [64], but are not shown here). The families are produced for $\sigma = 0$ in Eq. (6), $\gamma = 1/2$ in Eq. (7), and fixed propagation constant, $b = -10$. The fundamental and dipole families merge at $\beta \approx 2.135$, while the tripole and quadrupole ones merge at $\beta \approx 3.565$. (c) The critical ("upper") value, β_{upp}^d , at which the fundamental and dipole branches merge, vs. the propagation constant, b . Curve $\beta_{\text{upp}}^q(b)$ shows the same for the merger of the tripole and quadrupole branches.

This solution exists for all values of the control parameters, β_0 and σ , except for $\sigma = 0$. Further, Eq. (11) with σ and $R(x, y)$ taken in the form of Eqs. (13) and (15), where $\Gamma = 0$ is again fixed, also gives rise to an exact solution:

$$W(x, y) = W_0 \exp\left(-\frac{1}{2}r^2 - \frac{1}{2}i\beta_0 xy\right), \quad (20)$$

this time with

$$W_0^2 = \frac{1}{2\sigma} \left(1 - \left(\frac{\beta_0}{2}\right)^2\right), \quad b = -\left[1 + \frac{1}{2\sigma} \left(1 - \left(\frac{\beta_0}{2}\right)^2\right)\right]. \quad (21)$$

This solution exists if Eq. (21) yields $W_0^2 > 0$, i.e., $\beta_0 < 2$ and $\sigma > 0$.

Another exact solution of Eq. (11), with σ and $R(x, y)$ again taken in the form of Eqs. (13) and (15), exists under the special condition,

$$\beta_0 = 2, \sigma = 0, \Gamma = 0. \quad (22)$$

This solution is also found in the form of ansatz (20), precisely with $\frac{1}{2}\beta_0$ replaced by 1, as per Eq. (22). However, unlike the solution represented by Eqs. (20) and (21), this time it is not a single one, but a *continuous family* of exact solutions, with *arbitrary amplitude* W_0 , and propagation constant

$$b = -(1 + W_0^2). \quad (23)$$

The possibility to obtain the continuous family of the exact 2D solitons, instead of an isolated one, is a compensation for selecting the special values of the parameters, as fixed by Eq. (22).

The exact solutions clearly suggest that the quasi-1D model, based on Eq. (14), features the unbreakable \mathcal{PT} symmetry, as the respective solution, given by Eqs. (18) and (19), exists for an arbitrarily large strength of the gain-loss term, β_0 . On the other hand, the full 2D model, based on Eq. (15), gives rise to the exact solutions, in the form of Eqs. (20), (21) or (22), (23), which exist only at $\beta_0 \leq 2$, hence the unbreakability of the \mathcal{PT} symmetry is not guaranteed in the latter case.

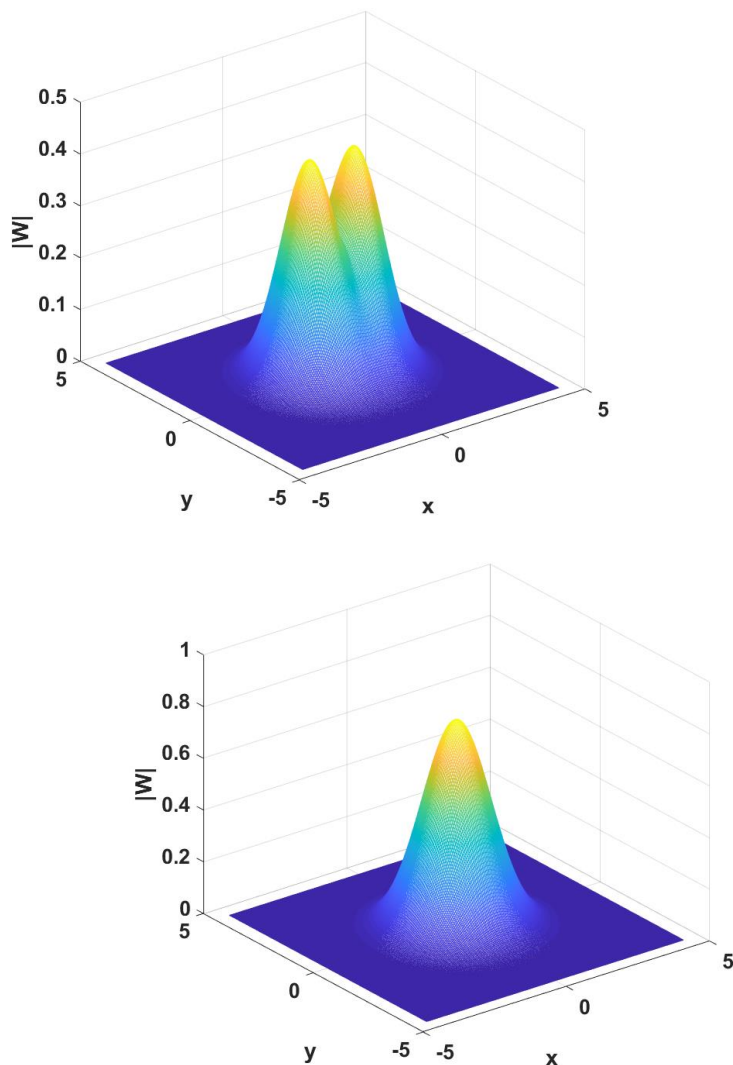


FIG. 6: Typical examples of 2D \mathcal{PT} -symmetric solitons produced by the model with the quasi-1D gain-loss profile defined by Eq. (14). The top and bottom panels display, severally, a stable single-peak soliton with propagation constant $b = -2$, and an unstable dual-peak one with $b = -2.7$. In both cases, other parameters are $\beta_0 = 0.8$, $\sigma = 1$, and $\Gamma = 0$.

B. Numerical results

1. The quasi-1D model

The exact solution of the model with the quasi-1D gain-loss modulation, given by Eqs. (18) and (19) can be embedded into a family of solitons produced by a numerical solution of Eq. (17), with $S(r)$ and $R(x, y)$ taken as per Eqs. (13) and (14), respectively (the latter is taken here with $\Gamma = 0$). The stationary 2D solutions were constructed by means of the Newton's conjugate gradient method. Then, the stability of the stationary states was identify by numerical computation of eigenvalues of small perturbations, using linearized equations for perturbations around the stationary solitons. This computation was performed with the help of the spectral collocation method. Finally, the stability prediction, based on the eigenvalues, was verified through direct simulations of the perturbed evolution of the solitons.

Generic examples of numerically found stable and unstable solitons, which may have single- and dual-peak shapes, are shown in Fig. 6. In accordance with these examples, all the double-peak solitons are unstable, and almost all the single-peak ones are stable. In particular, all the exact solutions, given by Eqs. (18) and (19), are found to be stable.

Results of the stability analysis for the \mathcal{PT} -symmetric solitons in the model with the quasi-1D shape of the gain-loss term, based on the eigenvalue computation, are summarized by the stability chart in the plane of (b, β_0) , i.e., the

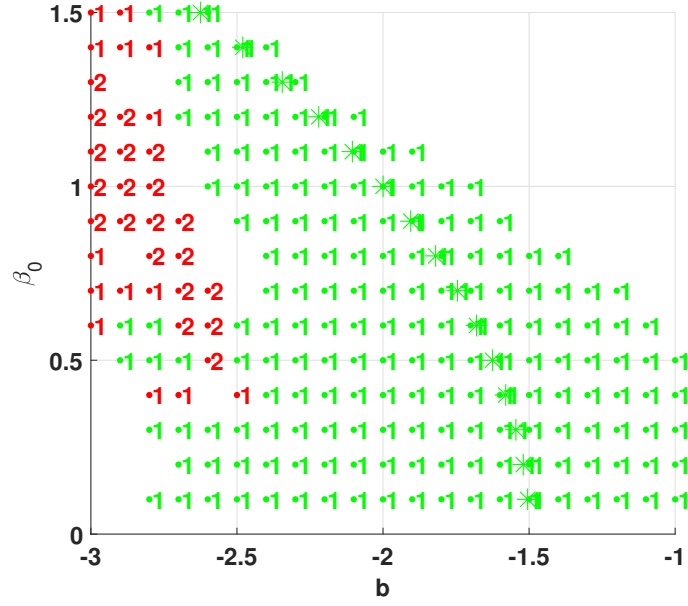


FIG. 7: (Color online) The stability chart for the solitons supported by quasi-1D \mathcal{PT} -symmetric gain-loss profile (14) with $\Gamma = 0$, in the case of $\sigma = 1$ in Eq. (13). Exact soliton solutions, given by Eqs. (18) and (19), are indicated by stars (they all are stable), while stable and unstable numerically found solitons are shown by green and red dots, respectively. Numbers near the dots denote the number of peaks in each soliton (one or two). No soliton solutions were found in white areas.

soliton's propagation constant and strength of the gain-loss term in Eq. (14), which is displayed in Fig. 7. Direct simulations completely corroborate the predictions produced by the stability eigenvalues. In particular, the solitons which are predicted to be unstable get destructed, decaying in the course of the perturbed evolution. This figure corroborates the unbreakable character of the \mathcal{PT} symmetry in the model, as the stability region does not exhibit a boundary at large values of β_0 .

The stability chart, drawn in Fig. 7 for $\sigma = 1$ in Eq. (13), is quite similar to its counterparts produced at other values of $\sigma > 0$. The situation is different in the case of $\sigma = 0$, when the exact solution given by Eqs. (18) and (19) does not exist. The respective stability chart, displayed in Fig. 8, demonstrates essential differences from the one in Fig. 7: the stability area is conspicuously smaller, all unstable solutions, as well as stable ones, featuring the single-peak shape.

2. The full 2D model

A drastic difference produced by the stability analysis for exact solutions of the full 2D model, given by Eqs. (20) and (21) for $\sigma > 0$, $\Gamma = 0$ and arbitrary β_0 , and by Eq. (23) for the special case (22), is that these solutions are completely *unstable*. Furthermore, all numerical solutions found in the full 2D model with $\Gamma = 0$ in Eq. (15) are unstable too. The stabilization in this model may be provided by $\Gamma > 0$, i.e., by confining the spatial growth of the local gain and loss in Eq. (15). For fixed σ , there is a minimum value Γ_{\min} of Γ which provides for the stabilization. In fact, Γ_{\min} depends on the size of the solution domain: in an extremely large domain, one may find very broad solitons, i.e., ones with very small b (see Eq. (17)), at any $\Gamma > 0$. Practically speaking, the size of the domain is always finite, as the steep growth of $S(r)$, defined as per Eq. (13), cannot extend to infinity. As shown in Refs. [67]-[76], it is sufficient to secure the adopted modulation profile of $S(r)$ on a scale which is essentially larger than a characteristic size of the soliton supported by this profile. Thus, we have concluded that, for instance, in the domain of size $|x|, |y| \leq 9$ the solitons are stable in the model with $\sigma = 1$ in Eq. (13) at $\Gamma \geq 0.2$ in Eq. (15), being explicitly unstable, e.g., at $\Gamma = 0.1$. Typical examples of the stability charts for the \mathcal{PT} -symmetric solitons, numerically produced in the full 2D model with $\beta > 0$, are displayed in Fig. 9. Naturally, the stability area expands with the increase of Γ . It is worthy to note that Fig. 9(b) clearly suggests that the \mathcal{PT} symmetry in the model with the full 2D modulation of the gain-loss term may also be unbreakable, as the stability chart does features no upper boundary.

These charts include unstable and (very few) stable solitons with multi-peak shapes. Indeed, taking larger Γ , i.e., stronger confinement of the gain and loss in Eq. (15), it is possible to find *stable* multi-peak solitons with rather complex shapes, an example being a stable four-peak soliton displayed in Fig. 10 for $\Gamma = 0.5$.

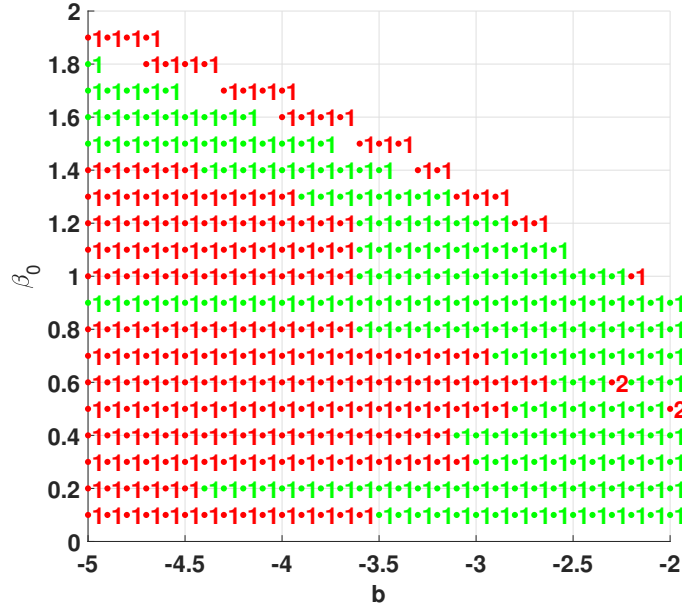


FIG. 8: The same as in Fig. 7 (the stability chart for \mathcal{PT} -symmetric solitons), but for $\sigma = 0$ in Eq. (13). Note an essential reduction of the stability area in comparison with its counterpart in Fig. 7.

The results for the quasi-1D and full 2D systems, reported in this section, do not provide an exhaustive analysis of these models. A comprehensive analysis, including, in particular, the consideration of possible solitons with embedded vorticity, will be presented elsewhere.

V. CONCLUSION

The objective of this article is to summarize theoretical results which demonstrate the stabilization of the \mathcal{PT} symmetry in both linear and nonlinear systems, making it possible to produce \mathcal{PT} -symmetric states at arbitrarily large values of the strength of the gain-loss terms in the system, i.e., of the coefficient in front of the non-Hermitian part of the underlying \mathcal{PT} -symmetric Hamiltonian. In Sections II and III, we have surveyed previously reported results obtained in two altogether different settings. Namely, the possibility of the restoration and complete stabilization of the \mathcal{PT} symmetry in the linear nanophotonic model of the waveguiding channel with a subwavelength width, the analysis of which is based on the full system of the Maxwell's equations, was recapitulated in Section II. The full stabilization, i.e., removal of the symmetry-breaking transition, takes place in the deeply subwavelength region. In Section III we have summarized results concerning the possibility of finding stable 1D solitons supported by the model with arbitrarily large values of the gain-loss coefficient, where the self-trapping of the solitons is provided by the self-defocusing nonlinearity with the local strength growing fast enough from the center to periphery. The model admits a particular exact solution for the fundamental soliton, the families of both fundamental and dipole modes being entirely stable.

Section IV has presented new results for the unbreakable \mathcal{PT} -symmetric solitons in two 2D extensions of the 1D model, *viz.*, with the quasi-1D and full 2D modulation profiles of the local gain-loss coefficient. These models also admit particular exact solutions, this time for 2D solitons. As a result, it is found the quasi-1D model readily gives rise to the stable family of fundamental (single-peak) 2D solitons for an arbitrarily large strength of the gain-loss term, while dual-peak ones are unstable. On the other hand, the stability of the solitons in the model with the full 2D \mathcal{PT} symmetry requires to impose spatial confinement on the gain-loss term. Further results for the 2D models will be presented elsewhere.

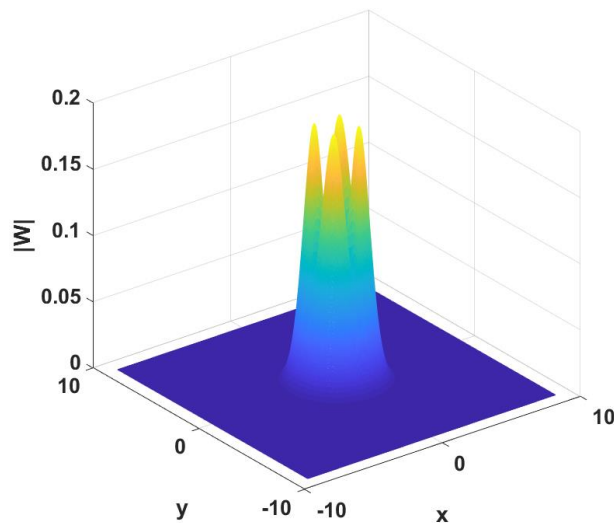


FIG. 10: An example of a stable \mathcal{PT} -symmetric four-peak soliton with propagation constant $b = -3$, found in the full 2D models with $\sigma = 1$ in Eq. (13) and $\Gamma = 0.5$ in Eq. (15).

- [4] C. M. Bender, D. C. Brody, and H. F. Jones, Complex extension of quantum mechanics, *Phys. Rev. Lett.* **89**, 270401 (2002).
- [5] C. M. Bender, Making sense of non-Hermitian Hamiltonians, *Rep. Prog. Phys.* **70**, 947-1018 (2007).
- [6] C. M. Bender, Rigorous backbone of \mathcal{PT} -symmetric quantum mechanics, *J. Phys. A: Math. Theor.* **49**, 401002 (2016).
- [7] K. G. Makris, R. El-Ganainy, D. N. Christodoulides, and Z. H. Musslimani \mathcal{PT} symmetric periodic optical potentials, *Int. J. Theor. Phys.* **50**, 1019-1041 (2011).
- [8] N. Moiseyev, *Non-Hermitian Quantum Mechanics*, (Cambridge University Press, 2011).
- [9] D. A. Zezyulin, I. V. Barashenkov, and V. V. Konotop, Stationary through-flows in a Bose-Einstein condensate with a \mathcal{PT} -symmetric impurity, *Phys. Rev. A* **94**, 063649 (2016).
- [10] I. V. Barashenkov, D. A. Zezyulin, and V. V. Konotop, Jamming anomaly in \mathcal{PT} -symmetric systems, *New J. Phys.* **18**, 075015 (2016).
- [11] I. V. Barashenkov and M. Gianfreda, An exactly solvable \mathcal{PT} -symmetric dimer from a Hamiltonian system of nonlinear oscillators with gain and loss, *J. Phys. A* **47**, 282001 (2014).
- [12] I. V. Barashenkov, Hamiltonian formulation of the standard \mathcal{PT} -symmetric nonlinear Schrödinger dimer, *Phys. Rev. A* **90**, 045802 (2014).
- [13] A. Ruschhaupt, F. Delgado, and J. G. Muga, Physical realization of \mathcal{PT} -symmetric potential scattering in a planar slab waveguide, *J. Phys. A: Math. Gen.* **38**, L171-L176 (2005).
- [14] R. El-Ganainy, K. G. Makris, D. N. Christodoulides, and Z. H. Musslimani, Theory of coupled optical \mathcal{PT} -symmetric structures, *Opt. Lett.* **32**, 2632-2634 (2007).
- [15] Z. H. Musslimani, K. G. Makris, R. El-Ganainy, and D. N. Christodoulides, Optical solitons in \mathcal{PT} periodic potentials, *Phys. Rev. Lett.* **100**, 030402 (2008).
- [16] M. V. Berry, Optical lattices with \mathcal{PT} -symmetry are not transparent, *J. Phys. A: Math. Theor.* **41**, 244007 (2008).
- [17] S. Klaiman, U. Günther, and N. Moiseyev, Visualization of branch points in \mathcal{PT} -Symmetric Waveguides, *Phys. Rev. Lett.* **101**, 080402 (2008).
- [18] S. Longhi, Bloch oscillations in complex crystals with \mathcal{PT} symmetry, *Phys. Rev. Lett.* **103**, 123601 (2009).
- [19] D. A. Zezyulin, Y. V. Kartashov, and V. V. Konotop, Stability of solitons in \mathcal{PT} -symmetric nonlinear potentials, *EPL* **96**, 64003 (2011).
- [20] R. Driben and B. A. Malomed, Stability of solitons in parity-time-symmetric couplers, *Opt. Lett.* **36**, 4323-4325 (2011).
- [21] N. V. Alexeeva, I. V. Barashenkov, A. A. Sukhorukov, and Y. S. Kivshar, Optical solitons in \mathcal{PT} -symmetric nonlinear couplers with gain and loss, *Phys. Rev. A* **85**, 063837 (2012).
- [22] M.-A. Miri, A. B. Aceves, T. Kottos, V. Kovanis, and D. N. Christodoulides, Bragg solitons in nonlinear \mathcal{PT} -symmetric periodic potentials, *Phys. Rev. A* **86**, 033801 (2012).
- [23] S. Nixon, L. Ge, and J. Yang, Stability analysis for solitons in \mathcal{PT} -symmetric optical lattices, *Phys. Rev. A* **85**, 023822 (2012).
- [24] J. D'Ambroise, P. G. Kevrekidis, and B. A. Malomed, Staggered parity-time-symmetric ladders with cubic nonlinearity, *Phys. Rev. E* **91**, 033207 (2015).
- [25] N. V. Alexeeva, I. V. Barashenkov, and Y. S. Kivshar, Solitons in \mathcal{PT} -symmetric ladders of optical waveguides, *New J. Phys.* **19**, 113032 (2017).
- [26] Y. Kominis, T. Bountis, and S. Flach, Stability through asymmetry: Modulationally stable nonlinear supermodes of

- asymmetric non-Hermitian optical couplers, Phys. Rev. **95**, 063832 (2017).
- [27] A. Guo, G. J. Salamo, D. Duchesne, R. Morandotti, M. Volatier-Ravat, V. Aimez, G. A. Siviloglou, and D. N. Christodoulides, Observation of \mathcal{PT} -symmetry breaking in complex optical potentials, Phys. Rev. Lett. **103**, 093902 (2009).
- [28] C. E. Rüter, K. G. Makris, R. El-Ganainy, D. N. Christodoulides, M. Segev, and D. Kip, Observation of parity-time symmetry in optics. *Nature Phys.* **6**, 192-195 (2010).
- [29] A. Regensburger, C. Bersch, M. A. Miri, G. Onishchukov, D. N. Christodoulides, and U. Peschel, Parity-time synthetic photonic lattices, *Nature* **488**, 167-171 (2012).
- [30] M. Wimmer, A. Regensburger, M. A. Miri, C. Bersch, D. N. Christodoulides, and U. Peschel, Observation of optical solitons in \mathcal{PT} -symmetric lattices, *Nature Commun.* **6**, 7782 (2015).
- [31] G. Castaldi, S. Savoia, V. Galdi, A. Alù, A. and N. Engheta, \mathcal{PT} metamaterials via complex-coordinate transformation optics, Phys. Rev. Lett. **110**, 173901 (2013).
- [32] H. Hodaei, M. A. Miri, M. Heinrich, D. N. Christodoulides, and M. Khajavikhan, Parity-time-symmetric microring lasers, *Science* **346**, 975-978 (2014).
- [33] S. Longhi, \mathcal{PT} -symmetric laser absorber, Phys. Rev. A **82**, 031801 (2010).
- [34] B. Peng, Ş. K. Özdemir, W. Chen, F. Nori, and L. Yang, Parity-time-symmetric whispering gallery microcavities, *Nature Phys.* **10**, 394-398 (2014).
- [35] Z. Zhang, Y. Zhang, J. Sheng, L. Yang, M. A. Miri, D. N. Christodoulides, B. He, Y. Zhang, and M. Xiao, Observation of parity-time symmetry in optically induced atomic lattices, Phys. Rev. Lett. **117**, 123601 (2016).
- [36] J.-Y. Lien, Y.-N. Chen, N. Ishida, H.-B. Chen, C.-C. Hwang, and F. Nori, Multistability and condensation of exciton-polaritons below threshold, Phys. Rev. B **91**, 024511 (2015).
- [37] T. Gao, E. Estrecho, K. Y. Bliokh, T. C. H. Liew, M. D. Fraser, S. Brodbeck, M. Kamp, C. Schneider, S. Höfling, Y. Yamamoto, F. Nori, Y. S. Kivshar, A. G. Truscott, R. G. Dall, and E. A. Ostrovskaya, Observation of non-Hermitian degeneracies in a chaotic exciton-polariton billiard, *Nature* **526**, 554-558 (2015).
- [38] I. Yu. Chestnov, S. S. Demirchyan, A. P. Alodjants, Y. G. Rubo, and A. V. Kavokin, Permanent Rabi oscillations in coupled exciton-photon systems with \mathcal{PT} -symmetry, *Sci. Rep.* **6**, 19551 (2016).
- [39] H. Ramezani, T. Kottos, R. El-Ganainy, and D. N. Christodoulides, Unidirectional nonlinear \mathcal{PT} -symmetric optical structures, Phys. Rev. A **82**, 043803 (2010).
- [40] X. Zhu, H. Ramezani, C. Shi, J. Zhu, and X. Zhang, \mathcal{PT} -Symmetric Acoustics, Phys. Rev. X **4** 031042 (2014); R. Fleury, D. Sounas, and A. Alú, An invisible acoustic sensor based on parity-time symmetry, *Nature Communications* **6**, 5905 (2015).
- [41] X.-W. Xu, Y.-x. Liu, C.-P. Sun, and Y. Li, Mechanical \mathcal{PT} symmetry in coupled optomechanical systems, Phys. Rev. A **92** 013852 (2015).
- [42] L. Schwarz, H. Cartarius, Z. H. Musslimani, J. Main, and G. Wunner, Vortices in Bose-Einstein condensates with \mathcal{PT} -symmetric gain and loss, Phys. Rev. **95**, 053613 (2017).
- [43] J. M. Lee, T. Kottos, and B. Shapiro, Macroscopic magnetic structures with balanced gain and loss, Phys. Rev. B **91**, 094416 (2015).
- [44] E. Destyl, S. P. Nuiro, D. E. Pelinovsky, and P. Poulet, Coupled pendula chains under parametric \mathcal{PT} -symmetric driving force, Phys. Lett. A **381**, 3884 -3892 (2017).
- [45] J. Schindler, Z. Lin, J. M. Lee, H. Ramezani, F. M. Ellis, and T. Kottos, *J. Phys. A: Math. Theor.* **45**, 444029 (2012).
- [46] C. M. Bender, D. C. Brody, and J.-H. Chen, \mathcal{PT} -symmetric extension of the Korteweg-de Vries equation, *J. Phys. A: Math. Theor.* **40**, F153-F160 (2007).
- [47] A. Fring, \mathcal{PT} -symmetric deformations of the Korteweg-de Vries equation, *ibid.* **40**, 4215-4334 (2007);
- [48] Z. Y. Yan, Complex \mathcal{PT} -symmetric nonlinear Schrödinger equation and Burgers equation, *Phil. Trans. Roy. Soc. A - Math Phys. Eng. Sci.* **371**, 20120059 (2013).
- [49] J. Cuevas-Maraver, B. Malomed, and P. Kevrekidis, A \mathcal{PT} -symmetric dual-core system with the sine-Gordon nonlinearity and derivative coupling, *Symmetry* **8**, 39 (2016).
- [50] H. Sakaguchi and B. A. Malomed, One- and two-dimensional solitons in \mathcal{PT} -symmetric systems emulating spin-orbit coupling, *New J. Phys.* **18**, 105005 (2016).
- [51] V. V. Konotop, J. Yang, and D. A. Zezyulin, Nonlinear waves in \mathcal{PT} -symmetric systems, *Rev. Mod. Phys.* **88**, 035002 (2016).
- [52] S. V. Suchkov, A. A. Sukhorukov, J. H. Huang, S. V. Dmitriev, C. Lee, and Y. S. Kivshar, Nonlinear switching and solitons in \mathcal{PT} -symmetric photonic systems, *Laser and Photonics Reviews* **10**, 177-213 (2016).
- [53] X. Zhu, H. Wang, H. Li, W. He, and Y. He, Two-dimensional multipeak gap solitons supported by parity-time-symmetric periodic potentials, *Opt. Lett.* **38**, 2723-2725 (2013).
- [54] G. Burlak and B. A. Malomed, Stability boundary and collisions of two-dimensional solitons in \mathcal{PT} -symmetric couplers with the cubic-quintic nonlinearity, *Phys. Rev. E* **88**, 062904 (2013).
- [55] J. Yang, Partially \mathcal{PT} -symmetric optical potentials with all-real spectra and soliton families in multidimensions, *Opt. Lett.* **39**, 1133-1136 (2014).
- [56] X. Ren, H. Wang, H. Wang, and Y. He, Stability of in-phase quadruple and vortex solitons in the parity-time-symmetric periodic potentials, *Opt. Exp.* **22**, 19774-19782 (2014).
- [57] Z. Chen, J. Liu, S. Fu, Y. Li, and B. A. Malomed, Discrete solitons and vortices on two-dimensional lattices of \mathcal{PT} -symmetric couplers, *Opt. Exp.* **22**, 29679-29692 (2014).

- [58] H. Wang, S. Shi, X. Ren, X. Zhu, B. A. Malomed, D. Mihalache, and Y. He, Two-dimensional solitons in triangular photonic lattices with parity-time symmetry, *Opt. Commun.* **335**, 146-152 (2015).
- [59] J. Yang, Necessity of \mathcal{PT} symmetry for soliton families in one-dimensional complex potentials, *Phys. Lett. A*, **378**, 367-373 (2014).
- [60] B. A. Malomed, Evolution of nonsoliton and “quasiclassical” wavetrains in nonlinear Schrödinger and Korteweg - de Vries equations with dissipative perturbations, *Physica D* **29**, 155-172 (1987).
- [61] E. V. Vanin, A. I. Korytin, A. M. Sergeev, D. Anderson, M. Lisak, and L. Vázquez, Dissipative optical solitons, *Phys. Rev. A* **49**, 2806-2811 (1994).
- [62] E. N. Tsoy, A. Ankiewicz, and N. Akhmediev, Dynamical models for dissipative localized waves of the complex Ginzburg-Landau equation, *Phys. Rev. E* **73**, 036621 (2006).
- [63] J. Yang, Symmetry breaking of solitons in one-dimensional parity-time-symmetric optical potentials, *Opt. Lett.* **39**, 5547-5550 (2014).
- [64] Y. V. Kartashov, B. A. Malomed, and L. Torner, Unbreakable \mathcal{PT} symmetry of solitons supported by inhomogeneous defocusing nonlinearity, *Opt. Lett.* **39**, 5641-5644 (2014).
- [65] T. Soloman Raju, T. Ashok Hedge, and C. N. Kumar, Unbreakable \mathcal{PT} symmetry of exact solitons in inhomogeneous nonlinear optical media, *J. Opt. Soc. Am. B* **33**, 35-40 (2016).
- [66] D. Guo, J. Xia, L. Gu, H. Jin, and L. Dong, One- and two-dimensional bright solitons in inhomogeneous defocusing nonlinearities with an antisymmetric periodic gain and loss, *Physica D* **343**, 1-6 (2017).
- [67] O. V. Borovkova, Y. V. Kartashov, B. A. Malomed, and L. Torner, Algebraic bright and vortex solitons in defocusing media, *Opt. Lett.* **36**, 3088-3090 (2011).
- [68] O. V. Borovkova, Y. V. Kartashov, L. Torner, and B. A. Malomed, Bright solitons from defocusing nonlinearities, *Phys. Rev. E* **84**, 035602 (R) (2011).
- [69] Q. Tian, L. Wu, Y. Zhang, and J.-F. Zhang, Vortex solitons in defocusing media with spatially inhomogeneous nonlinearity, *Phys. Rev. E* **85**, 056603 (2012).
- [70] Y. Wu, Q. Xie, H. Zhong, L. Wen, and W. Hai, Algebraic bright and vortex solitons in self-defocusing media with spatially inhomogeneous nonlinearity, *Phys. Rev. A* **87**, 055801 (2013).
- [71] W. B. Cardoso, J. Zeng, A. T. Avelar, D. Bazeia, and B. A. Malomed, Bright solitons from the nonpolynomial Schrödinger equation with inhomogeneous defocusing nonlinearities, *Phys. Rev. E* **88**, 025201 (2013).
- [72] R. Driben, Y. V. Kartashov, B. A. Malomed, T. Meier, and L. Torner, Soliton gyroscopes in media with spatially growing repulsive nonlinearity, *Phys. Rev. Lett.* **112**, 020404 (2014).
- [73] Y. V. Kartashov, B. A. Malomed, Y. Shnir, and L. Torner, Twisted toroidal vortex-solitons in inhomogeneous media with repulsive nonlinearity, *Phys. Rev. Lett.* **113**, 264101 (2014).
- [74] R. Driben, N. Dror, B. Malomed, and T. Meier, Multipoles and vortex multiplets in multidimensional media with inhomogeneous defocusing nonlinearity, *New J. Phys.* **17**, 083043 (2015).
- [75] Y. V. Kartashov, B. A. Malomed, V. A. Vysloukh, M. R. Belić, and L. Torner, Rotating vortex clusters in media with inhomogeneous defocusing nonlinearity, *Opt. Lett.* **42**, 446-449 (2017).
- [76] J. Zeng and B. A. Malomed, Localized dark solitons and vortices in defocusing media with spatially inhomogeneous nonlinearity, *Phys. Rev. E* **95**, 052214 (2017).
- [77] R. Zhong, Z. Chen, C. Huang, Z. Luo, H. Tan, B. A. Malomed, and Y. Li, Self-trapping under the two-dimensional spin-orbit-coupling and spatially growing repulsive nonlinearity, arXiv:1712.01430.
- [78] C. Huang, F. Ye, Y. V. Kartashov, B. A. Malomed, and X. Chen, \mathcal{PT} symmetry in optics beyond the paraxial approximation, *Opt. Lett.* **39**, 5443-5446 (2014).
- [79] C. H. Liang, D. D. Scott, and Y. N. Joglekar, \mathcal{PT} restoration via increased loss and gain in the \mathcal{PT} -symmetric Aubry-André model, *Phys. Rev. A* **89**, 030102(R) (2014).
- [80] Y. Lumer, Y. Plotnik, M. C. Rechtsman, and M. Segev, Nonlinearly induced \mathcal{PT} transition in photonic systems, *Phys. Rev. Lett.* **111**, 263901 (2013).